

Dynamical spectrum via determinant-free linear algebra

Joseph Horan

Abstract. We consider a sequence of matrices that are associated to Markov dynamical systems and use determinant-free linear algebra techniques (as well as some algebra and complex analysis) to rigorously estimate the eigenvalues of every matrix simultaneously without doing any calculations on the matrices themselves. As a corollary, we obtain mixing rates for every system at once, as well as symmetry properties of densities associated to the system; we also find the spectral properties of a sequence of related factor systems.

Introduction Consider, for the time being, a *stochastic* d -by- d matrix P . The matrix P represents a finite-dimensional *Markov chain*, a stochastic model where states transition to one another with some probability at discrete time steps according to the entries in the matrix. Thus, if at time 0 the probabilities of being in each of the d states are given by the vector x , then the probabilities of being in each of the d states at time 1 are given by Px (P acting on x); see Figure 1. The asymptotic properties of the Markov chain, such as what the stationary distribution is (if it exists) and the rate at which the process converges to that distribution, are determined by the spectral theory of the matrix P . Some linear algebra, potentially including some numerical computation, then allows us to compute these desired quantities. In particular, in the case that the Markov chain is *mixing*, we wish to find the modulus of the second-largest eigenvalue(s), which tells us the rate at which the Markov chain converges to its stationary distribution: the mixing time is at most proportional to the reciprocal of the logarithm of the modulus of the second-largest eigenvalue.¹

In the field of dynamical systems, we often start with a map T on some state space X , and we want to answer questions such as “what happens to most of the orbits of T over a long time?” and “do regions of X mix together over time, and at what rate?” These questions are less about looking at individual orbits of points under T and more

¹For the proof of this fact and for more on Markov chains, see the book by Levin, Peres, and Wilmer [7]; applications include statistical mechanics and Markov chain Monte Carlo (MCMC).

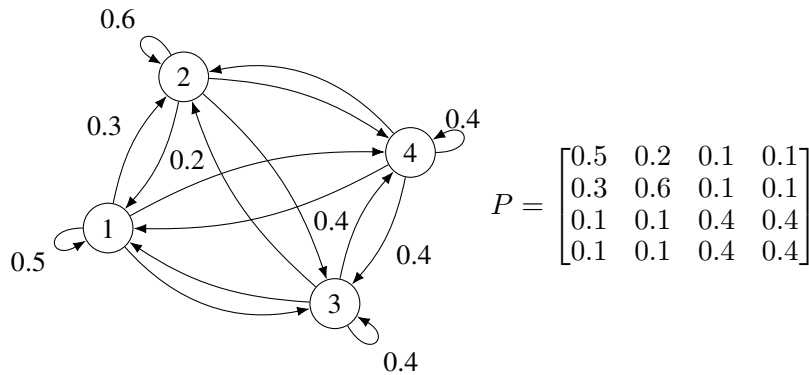


Figure 1. A Markov chain with four states and its associated transition matrix.

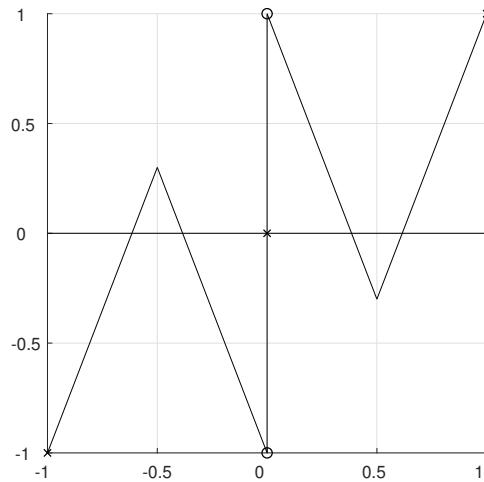


Figure 2. The paired tent map, with parameter $\kappa = 0.3$.

about looking at what happens *on average*. Specifically, we can learn much about the dynamical system (X, T) by studying how *probability densities* on X change over time under the action of T .

To formalize this process and to lead into the focus of this article, we consider a specific class of piecewise linear maps acting on $[-1, 1]$.

Definition. Define $T_\kappa : [-1, 1] \rightarrow [-1, 1]$ by:

$$T_\kappa(x) = \begin{cases} 2(1 + \kappa)(x + 1) - 1, & x \in [-1, -1/2], \\ -2(1 + \kappa)x - 1, & x \in [-1/2, 0), \\ 0, & x = 0, \\ -2(1 + \kappa)x + 1, & x \in (0, 1/2], \\ 2(1 + \kappa)(x - 1) + 1, & x \in [1/2, 1]. \end{cases}$$

We call T_κ a *paired tent map*, because there are two tents paired together. See Figure 2 for an illustration.²

Let f be a probability density on $[-1, 1]$; that is, a non-negative measurable function defined on $[-1, 1]$ with integral equal to 1. As a rough analogy, one could imagine that the space $[-1, 1]$ is a bowl of banana bread batter into which one has placed chocolate chips, and f is the density of chocolate chips. Applying the map T_κ stirs the space up, moving the chocolate chips around; there is then a new density, call it $P_\kappa f$, that describes the new locations of the chocolate chips. Some parts of the batter may have more chocolate chips than before, and some fewer, but the total amount of chocolate chips has not changed. It turns out that the operator P_κ can be defined on all integrable functions (that is, on $L^1(\lambda)$, where λ is the normalized Lebesgue measure), and is bounded and linear; we call P_κ the *Perron-Frobenius operator associated to T_κ* .³ It also turns out that there is an invariant subspace for P_κ of L^1 called BV (short for

²In general, the tents could be different; see Section 4 of [5].

³To be rigorous, $P_\kappa f$ is the Radon-Nikodym derivative of the measure $A \mapsto \lambda(f \mathbb{1}_{T^{-1}(A)})$, which exists because T_κ is a non-singular map. See, for example, Chapter 4 of [3].

bounded variation) on which the spectrum of P_κ is well-behaved, and so we restrict our focus to BV for the remainder of this article.⁴

Returning to the questions posed above, we note that P_κ is the infinite-dimensional analogue of the transition matrix P for the Markov chain. If we want to find a “stationary distribution” for T_κ , we really are looking for invariant densities, which are eigenvectors of P_κ with eigenvalue 1. If all initial densities converge to an invariant density over time, then we have a good idea of where most of the points in $[-1, 1]$ end up in the long run: no matter where they started, points will be distributed over $[-1, 1]$ according to the invariant density. Moreover, if there is a gap in modulus between an eigenvalue of 1 and the rest of the spectrum, this gap describes how quickly this convergence occurs, in the same way as described above for Markov chains.

By inspection, if $\kappa = 0$, then from the graph of T_κ it is clear that T_κ has *two* invariant densities: the characteristic functions on $[-1, 0]$ and $[0, 1]$, respectively. If $\kappa > 0$, we can see that these two densities are no longer invariant, because there is mixing between the two intervals $[-1, 0]$ and $[0, 1]$. It is *a priori* unclear whether or not T_κ has an invariant density, and if it does whether it has a spectral gap; however, to answer these questions we can study P_κ , as described above.

Markov Maps and Partitions Unfortunately, the fact that P_κ is not a matrix complicates things; at first glance, we no longer have all of the computational and theoretical tools available to us previously. However, because T_κ is piecewise-linear, if the map T_κ has an additional property then we can recover a significant portion of our toolkit.

Definition. The map T_κ is *Markov* when there is a finite collection $\{R_i\}_{i=1}^r$ of disjoint open intervals in $[-1, 1]$ such that:

1. $[-1, 1] \setminus \bigcup_i R_i$ is the collection of endpoints of the intervals $\{R_i\}$, and
2. if R_i intersects $T_\kappa(R_j)$, then all of R_i is contained in $T_\kappa(R_j)$.

The collection $\{R_i\}$ is called a *Markov partition* for T_κ , even though it is not a partition, strictly speaking.

The next lemma is a combination of Theorem 9.2.1 in [3] and Lemma 3.1 in [2], stated in the specific case of our paired tent maps T_κ .

Lemma 1. Suppose that the paired tent map T_κ is Markov, with Markov partition $\{R_i\}_{i=1}^r$. If $V = \text{span}_{\mathbb{C}} \{\mathbb{1}_{R_i} : 1 \leq i \leq r\}$ and P_κ is the Perron-Frobenius operator for T_κ , then V is P_κ -invariant (considered as a subspace of BV). The adjacency matrix for T_κ is given by the r -by- r matrix $A_\kappa = [a_{ij}]$, where

$$a_{ij} = \begin{cases} 1, & R_i^o \subset T(R_j), \\ 0, & \text{otherwise.} \end{cases}$$

Define an isomorphism $\phi_r : V \rightarrow \mathbb{C}^r$ by $\phi(\mathbb{1}_{R_i}) = e_i$. Then the restriction of P_κ to V can be represented by the r -by- r matrix $M_\kappa = (2(1 + \kappa))^{-1} A_\kappa$, with $\phi_r \circ P_\kappa = M_\kappa \circ \phi_r$. Moreover,

$$\sigma(P_\kappa) \setminus \overline{B(0, (2(1 + \kappa))^{-1})} = (2(1 + \kappa))^{-1} \sigma(A_\kappa) \setminus \overline{B(0, (2(1 + \kappa))^{-1})}.$$

⁴As shown by Ding, Du, and Li [4], Perron-Frobenius operators can have L^1 -spectrum equal to the entire closed unit disk; the BV -spectrum is significantly more reasonable.

We see that when T_κ is Markov, to find the largest eigenvalues for P_κ it suffices to look only at the spectrum of the matrix A_κ , for which we have all of our linear algebra tools. In particular, we can look at the spectrum of A_κ to find the second-largest eigenvalues. So, we ask: when are these maps Markov? A general sufficient condition for piecewise linear maps is given by the following lemma, which says that it is enough for the endpoints of monotonicity intervals to be invariant in finitely many steps. We may then apply the lemma to T_κ by investigating the images of $\pm 1/2$. Recall that $T(x^+)$ is the limit $\lim_{y \rightarrow x^+} T(y)$, and similarly for $T(x^-)$.

Lemma 2. *Let $T : [a, b] \rightarrow [a, b]$ be an onto piecewise linear map, and let E_0 be the set of endpoints of the intervals of monotonicity for T . For each $i \geq 1$, let $E_i = \{T(s^\pm) : s \in E_{i-1}\}$. Suppose that there exists m such that $E_m = E_{m+1}$. Then T is Markov, with Markov partition $\{R_i\}_{i=1}^R$, where $\{r_i\}_{i=0}^M$ enumerates E_m in an increasing way and $R_i = (r_{i-1}, r_i)$.*

Proof. Let m be the smallest m such that $E_m = E_{m+1}$; let r_i and R_i be defined as in the statement of the lemma. Since the union of the intervals $\{R_i\}$ and their endpoints is the same as the union of the intervals of monotonicity along with those endpoints, $[-1, 1] \setminus \bigcup_i R_i$ is the endpoints of the R_i . Then, since $E_m = E_{m+1}$, for each j we have $T(R_j) = (r_k, r_l)$ for some $k < l$ depending on j . Thus, if $R_i \cap T(R_j) \neq \emptyset$, we must have $k \leq i < l$, since the intervals R_i are disjoint; hence $R_i \subset T(R_j)$. Hence T is Markov. ■

Lemma 3. *There exists a decreasing sequence $(\kappa_n)_{n=1}^\infty \subset (0, 1/2)$ such that T_{κ_n} is Markov and $\kappa_n \xrightarrow{n \rightarrow \infty} 0$. Each κ_n satisfies $(2 + 2\kappa)^n \kappa = 1$. The Markov partition for T_{κ_n} is, for $n = 1$,*

$$\left\{ \left(-1, -\frac{1}{2}\right), \left(-\frac{1}{2}, -\kappa_1\right), \left(-\kappa_1, 0\right), \left(0, \kappa_1\right), \left(\kappa_1, \frac{1}{2}\right), \left(\frac{1}{2}, 1\right) \right\}$$

and for $n \geq 2$,

$$\begin{aligned} & \left\{ \left(-1, T_{\kappa_n}(-\kappa_n)\right) \right\} \cup \left\{ \left(T_{\kappa_n}^i(-\kappa_n), T_{\kappa_n}^{i+1}(-\kappa_n)\right) \right\}_{i=1}^{n-2} \\ & \cup \left\{ \left(T_{\kappa_n}^{n-1}(-\kappa_n), -\frac{1}{2}\right), \left(-\frac{1}{2}, -\kappa_n\right), \left(-\kappa_n, 0\right), \left(0, \kappa_n\right), \left(\kappa_n, \frac{1}{2}\right), \left(\frac{1}{2}, T_{\kappa_n}^{n-1}(\kappa_n)\right) \right\} \\ & \cup \left\{ \left(T_{\kappa_n}^{i+1}(\kappa_n), T_{\kappa_n}^i(\kappa_n)\right) \right\}_{i=1}^{n-2} \cup \left\{ \left(T_{\kappa_n}(\kappa_n), 1\right) \right\}. \end{aligned}$$

Remark. The Markov partitions for T_1 and T_4 , are shown in Figures 3a and 3b. The case $n = 1$ is distinct because the branch of the map used for $x = \kappa_n$ is different than the branches used for the further iterates $T_{\kappa_n}^i(\kappa_n)$. In each picture, one may visually confirm that the collection of intervals actually is a Markov partition by checking that the image of each (horizontal) interval stretches vertically over a union of consecutive intervals (at each endpoint, the graph of the map passes through intersection points of horizontal and vertical lines).

Proof. Consider the paired tent map T_κ for $\kappa \in (0, 1/2)$. We will use Lemma 2 to find conditions on κ that make T_κ Markov. Start with $E_0 = \{-1, -1/2, 0, 1/2, 1\}$. The map T_κ is continuous everywhere except at 0, for which the one-sided limits are ± 1 , and we have $T_\kappa(-1) = -1$ and $T_\kappa(1) = 1$. Then $T_\kappa(-1/2) = \kappa$ and $T_\kappa(1/2) = -\kappa$, so we consider iterates of κ under T_κ ; by symmetry, iterates of $-\kappa$ will work

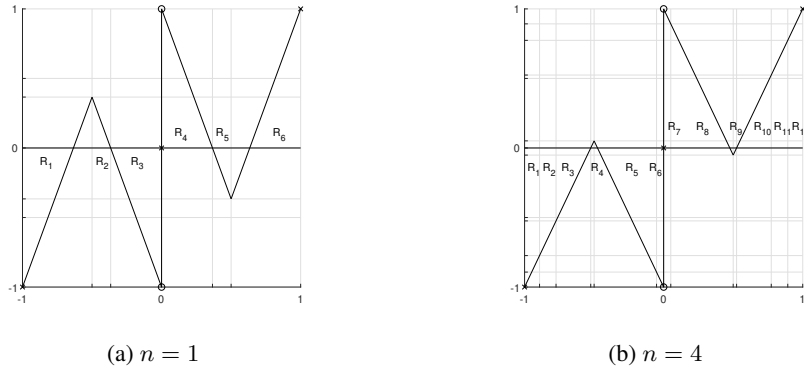


Figure 3. Markov partitions for T_{κ_n} , with $n = 1, 4$.

similarly. In particular, we will find, for each $n \geq 1$, a κ_n such that $T_{\kappa_n}^i(\kappa_n) = 1 - (2 + 2\kappa_n)^i \kappa_n > 1/2$ for $1 \leq i < n$ and

$$T_{\kappa_n}^n(\kappa_n) = 1 - (2 + 2\kappa_n)^n \kappa_n = 0.$$

First, consider the equation $(2 + 2\kappa)^n \kappa - 1 = 0$. Rearrange and take logarithms to obtain

$$n = h(\kappa) := \frac{-\log(\kappa)}{\log(2 + 2\kappa)}.$$

The function $h(\kappa)$ is decreasing on $(0, \infty)$, is unbounded as κ tends to 0, and has $h(1/2) = \log(2)/\log(3) < 1$. Thus we conclude that for each $n \in \mathbb{Z}_{\geq 1}$, there exists a unique $\kappa_n \in (0, 1/2)$ solving $(2 + 2\kappa)^n \kappa - 1 = 0$, and κ_n decreases to 0.⁵

Fix $n \geq 2$; we will show that $T_{\kappa_n}^i(\kappa_n) > 1/2$ for each $i = 1, \dots, n-1$. For each of those i , we have:

$$(2 + 2\kappa_n)^i \kappa_n = \frac{1}{(2 + 2\kappa_n)^{n-i}} \leq \frac{1}{2 + 2\kappa_n} < \frac{1}{2}.$$

Observe that for $i = 1$, we have

$$T_{\kappa_n}(\kappa_n) = 1 - (2 + 2\kappa_n)\kappa_n > \frac{1}{2}.$$

By repeated application of T_{κ_n} and use of the upper bound on $(2 + 2\kappa_n)^i \kappa_n$, we see that for all $1 \leq i < n$,

$$T_{\kappa_n}^i(\kappa_n) = 1 - (2 + 2\kappa_n)^i \kappa_n > \frac{1}{2}.$$

We have proven that $T_{\kappa_n}^n(\kappa_n) = 0$, and $T_{\kappa_n}^i(\kappa_n) > 1/2$ for $1 \leq i < n$; the symmetric statement holds for $-\kappa_n$.

Finally, fix $n \geq 1$. We claim that E_n is where the sequence of E_i terminates. To see this, observe that

$$E_n = E_0 \cup \{T_{\kappa_n}^i(\pm 1/2)\}_{i=1}^n = \{-1, -1/2, 0, 1/2, 1\} \cup \{T_{\kappa_n}^i(\pm \kappa_n)\}_{i=0}^{n-1},$$

⁵Another way to see this claim is by observing that $(n, \kappa) \mapsto T_{\kappa}^n(1/2)$ is increasing, in both n and κ (where this property makes sense).

$$\begin{bmatrix}
1 & 0 & 0 & & 0 & 0 & 0 & 1 & 0 & 0 & 0 & 0 & 0 & 0 \\
1 & 0 & 0 & & 0 & 0 & 1 & 0 & & & & & & \\
0 & 1 & 0 & & 0 & 0 & 1 & 0 & & & & & & \\
0 & 0 & 1 & & 0 & 0 & 1 & 0 & & & & & & \\
& \vdots & & \ddots & & & \vdots & & & & & & & \\
0 & 0 & 0 & & 1 & 0 & 1 & 0 & & & & & & \\
0 & 0 & 0 & & 1 & 0 & 1 & 0 & 0 & 0 & 0 & 0 & 0 & 0 \\
0 & 0 & 0 & & 1 & 0 & 1 & 0 & 0 & 1 & 1 & 0 & 0 & 0 \\
\hline
0 & 0 & 0 & & 0 & 1 & 1 & 0 & 0 & 1 & 0 & 1 & 0 & 0 \\
0 & 0 & 0 & & 0 & 0 & 0 & 0 & 0 & 1 & 0 & 1 & 0 & 0 \\
& & & & & & & & & 0 & 1 & 0 & 1 & 0 \\
& & & & & & & & & \vdots & & \ddots & & \vdots \\
& & & & & & & & & 0 & 1 & 0 & 0 & 1 & 0 & 0 \\
& & & & & & & & & 0 & 1 & 0 & 0 & 0 & 1 & 0 \\
& & & & & & & & & 0 & 1 & 0 & 0 & 0 & 0 & 1 \\
0 & 0 & 0 & & 0 & 0 & 0 & 0 & 0 & 1 & 0 & 0 & 0 & 0 & 0 & 1
\end{bmatrix}$$

Figure 4. General form of the $(2n + 4)$ -by- $(2n + 4)$ adjacency matrix A_n .

and note that we just saw that $T_{\kappa_n}^n(\pm\kappa_n) = 0$, so that $E_{n+1} = E_n$. This shows that T_{κ_n} is Markov, using Lemma 2. The listed Markov partitions are given by tracing $T_{\kappa_n}^i(\pm\kappa_n)$ as i runs from 0 to $n - 1$. ■

We now see that $T_n := T_{\kappa_n}$ is Markov for each $n \geq 1$. From the graph of the maps and the form of the Markov partition, it is easy to read off the adjacency matrix $A_n := A_{\kappa_n}$; since the partition has $2n + 4$ pieces, the matrix is $(2n + 4)$ -by- $(2n + 4)$. For $n \geq 4$ the general form of the matrix is as in Figure 4. For $n \leq 3$ some of the columns are combined.

The spectrum of $M_n := M_{\kappa_n}$ is just the spectrum of A_n scaled by $(2(1 + \kappa))^{-1}$, so we may focus our analysis on A_n . For each n , let

$$V_n = \text{span}_{\mathbb{C}} \{ \mathbf{1}_{R_i} : 1 \leq i \leq 2n + 4 \},$$

where $\{R_i\}$ is the Markov partition for T_n .

Spectral Properties of A_n Observe that the Markov partition for T_n is symmetric about 0. Moreover, observe that for any κ , T_κ is odd: $T_\kappa(-x) = -T_\kappa(x)$. In particular, if $\psi(x) = -x$, then $T_n \circ \psi = \psi \circ T_n$. The map ψ has a Perron-Frobenius operator, P_ψ , and the commutation relation says that $P_n P_\psi = P_\psi P_n$. We also see that the map ψ is Markov on the same partition as T_n , and noting the symmetry of this partition we obtain $\psi(R_i) = R_{2n+5-i}$. Thus the action of P_ψ on V_n is represented by the matrix J_n , as shown in Figure 5, and we have $M_n J_n = J_n M_n$, so also $A_n J_n = J_n A_n$. It is also clear that because $\psi^2 = \text{id}$, we have $J_n^2 = I$. Because $J_n^{-1} = J_n$, we have $J_n A_n J_n = A_n$. Left-multiplication by J_n reverses the order of the rows and right-multiplication by J_n reverses the order of the columns, so the combination of both of them is performing a half-circle rotation of the matrix; we thus have independent verification of the half-circle rotational symmetry of A_n , which could be seen from Figure 4.

$$\begin{bmatrix} 0 & 0 & 0 & & 0 & 0 & 1 \\ 0 & 0 & 0 & \dots & 0 & 1 & 0 \\ 0 & 0 & 0 & & 1 & 0 & 0 \\ & \vdots & & \ddots & & \vdots & \\ 0 & 0 & 1 & & 0 & 0 & 0 \\ 0 & 1 & 0 & \dots & 0 & 0 & 0 \\ 1 & 0 & 0 & & 0 & 0 & 0 \end{bmatrix}$$

Figure 5. The $(2n+4)$ -by- $(2n+4)$ matrix J_n .

Recall (see Theorem 1.3.19 in [6]) that if two diagonalizable matrices commute, then they are simultaneously diagonalizable, meaning that there is a shared basis of eigenvectors for the matrices. Also note that if two r -by- r matrices A and B commute, then \mathbb{C}^{2n+4} becomes a left- $\mathbb{C}[x, y]$ -module, by setting $p(x, y)v := p(A, B)v$ for polynomials $p(x, y) \in \mathbb{C}[x, y]$ and $v \in \mathbb{C}^{2n+4}$. We will now use these facts to find many spectral properties of A_n , using its relation with J_n ; note that we will find the spectral data of the entire sequence of A_n all at once! We use Axler's approach to determinant-free linear algebra [1] and the practical implementation of those ideas by McWorter and Meyers [8]. Moreover, we make significant use of the underlying map T_n to read off the algebraic relationships satisfied by A_n and J_n without doing a single matrix computation. We therefore reduce much of the study of the Perron-Frobenius operators to matrices that are easily studied by looking directly at the underlying maps.

Lemma 4. We have $A_n(A_n^{n+1} - 2A_n^n - 2J_n) = 0$.

Proof. Zooming in on the interval $[-1/2, 0]$, as in Figure 6, we can identify the intervals R_{n-1} through R_{n+2} . The interval R_{n-1} is the interval immediately to the left of the left zero of T_n in $[-1, 0]$; the interval R_n is the left branch of the leaking from $[-1, 0]$ to $[0, 1]$; the interval R_{n+1} is the large interval $(-1/2, -\kappa_n)$; and the interval R_{n+2} is the interval $(-\kappa_n, 0)$.

Looking at the map T_n and using the Markov partition, we see that for $i \leq n-1$, the interval R_{n+2} is mapped to R_1 and is subsequently expanded to the interval $(-1, r_i)$ in i total steps, which is represented by

$$A_n^i e_{n+2} = e_1 + \dots + e_i.$$

In the case of $i = n-1$, we have $T_n^{n-1}(R_{n+2}) = (-1, r_{n-1})$, and because r_{n-1} is the left zero for T_n in $[-1, 0]$, we have $T_n^n(R_{n+2}) = (-1, 0)$, which is represented by

$$A_n^n(e_{n+2}) = e_1 + \dots + e_{n+2}.$$

Then, we clearly have $T_n(-1, 0) = (-1, \kappa_n)$, so that because T_n is (except at $-1/2$) 2-to-1 on $[-1, 0]$, we have

$$A_n^{n+1} e_{n+2} = 2(e_1 + \dots + e_{n+3}) = 2A_n^n e_{n+2} + 2J_n e_{n+2},$$

where we used $J_n e_i = e_{2n+5-i}$. We rearrange this to $(A_n^{n+1} - 2A_n^n - 2J_n)e_{n+2} = 0$. Because A_n and J_n commute, we see that for any polynomial $p \in \mathbb{C}[x, y]$, we have

$$(A_n^{n+1} - 2A_n^n - 2J_n)p(A_n, J_n)e_{n+2} = 0.$$

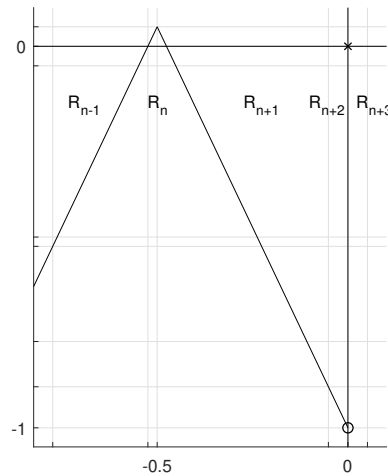


Figure 6. A zoomed-in look at the Markov partition for T_n in $[-1, 0]$.

Now, by the equations for $A_n^i e_{n+2}$, the fact that $J_n e_{n+2} = e_{n+3}$, and the fact that A_n and J_n commute, we see that

$$\begin{aligned} & \text{span}_{\mathbb{C}} \{p(A_n, J_n)e_{n+2} : p \in \mathbb{C}[x, y]\} \\ &= \text{span}_{\mathbb{C}} \{e_1, \dots, e_{n-1}, (e_n + e_{n+1}), e_{n+2}, \\ & \quad e_{n+3}, (e_{n+4} + e_{n+5}), e_{n+6}, \dots, e_{2n+4}\}. \end{aligned}$$

We can see that acting on the vector e_{n+2} by A_n and J_n does not separate e_n and e_{n+1} , or e_{n+4} and e_{n+5} , by observing that any image of an R_i either does not intersect R_n and R_{n+1} or covers both (and similarly for R_{n+4} and R_{n+5}). Moreover, this subspace does not contain the vectors $v_1 = e_1 + \dots + e_n - (e_{n+1} + e_{n+2})$ and $v_2 = J_n v_1$. These are two linearly independent vectors that both lie in the kernel of A_n ; to see they lie in the kernel, observe that the two vectors are representing $\mathbb{1}_{(-1, -1/2)} - \mathbb{1}_{(-1/2, 0)}$ and the reflection $\mathbb{1}_{(1/2, 1)} - \mathbb{1}_{(0, 1/2)}$, and the intervals stretch to the same image. All together, we now have a basis for \mathbb{C}^{2n+4} , every element of which is annihilated by $A_n(A_n^{n+1} - 2A_n^n - 2J_n)$, and hence $A_n(A_n^{n+1} - 2A_n^n - 2J_n) = 0$. ■

Let E^+ and E^- be the subspaces of symmetric and antisymmetric vectors in \mathbb{C}^{2n+4} , respectively.

Lemma 5. *For all $n \geq 1$, J_n is diagonalizable, with eigenspace E^+ corresponding to the eigenvalue 1 and eigenspace E^- corresponding to the eigenvalue -1 . Moreover, the eigenspaces E^\pm are A_n -invariant.*

Proof. We have $J_n^2 = I$, so that $(J_n - I)(J_n + I) = 0$. Since $J_n \pm I \neq 0$, we see that the minimal polynomial of J_n is

$$m_{J_n}(x) = x^2 - 1 = (x - 1)(x + 1),$$

and so J_n is diagonalizable (because the minimal polynomial is separable), with eigen-

values ± 1 . The projections onto the eigenspaces E_{+1} and E_{-1} are given by

$$\frac{J_n + I}{1 + 1} = \frac{1}{2}(I + J_n), \quad \frac{J_n - I}{-1 - 1} = \frac{1}{2}(I - J_n),$$

respectively, by normalizing the factor of the minimal polynomial that does not annihilate the appropriate space. This immediately shows that $E_{+1} = E^+$ and $E_{-1} = E^-$. Finally, A_n and J_n commute, so for $s \in E^+$ and $a \in E^-$ we have

$$J_n A_n s = A_n J_n s = A_n s, \quad J_n A_n a = A_n J_n a = -A_n a,$$

thus showing that E^\pm are A_n -invariant. ■

For notation, for all $n \geq 1$ let $f_n(x) = x^n(x - 2) - 2$, $g_n(x) = x^n(x - 2) + 2$, and $h_n(x, y) = x^n(x - 2) - 2y$.

Lemma 6. *The polynomials f_n and g_n are irreducible over $\mathbb{Q}[x]$, separable with no roots at zero, and do not share any roots.*

Proof. For irreducibility, apply Eisenstein's Criterion with $p = 2$ in both cases, followed by Gauss's Lemma. Since \mathbb{Q} is characteristic zero, f_n and g_n are both separable. Clearly 0 is not a root of either polynomial, and since $f_n(x) = g_n(x) - 4$, the two polynomials cannot share any roots. ■

Proposition 7. *Let $n \geq 1$. We have:*

1. *the kernel of A_n is $\ker(A_n) = \text{span}_{\mathbb{C}}\{v_1 + J_n v_1\} \oplus \text{span}_{\mathbb{C}}\{v_1 - J_n v_1\}$, for $v_1 = e_1 + \cdots + e_n - (e_{n+1} + e_{n+2})$;*
2. *for $s \in E^+$, $h(A_n, J_n)s = f_n(A_n)s$, and the minimal polynomial of A_n restricted to E^+ is $xf_n(x)$;*
3. *for $a \in E^-$, $h(A_n, J_n)a = g_n(A_n)a$, and the minimal polynomial of A_n restricted to E^- is $xg_n(x)$;*
4. *the minimal polynomial of A_n is*

$$m_{A_n}(x) = xf_n(x)g_n(x) = x(x^{2n+2} - 4x^{2n+1} + 4x^{2n} - 4);$$

5. *the characteristic polynomial of A_n is $\chi_{A_n}(x) = xm_{A_n}(x)$;*
6. *A_n is diagonalizable over \mathbb{C} , with all eigenvectors corresponding to roots of f_n being symmetric and all eigenvectors corresponding to roots of g_n being antisymmetric.*

Proof. First, we have already seen (in the proof of Lemma 4) that v_1 and $J_n v_1$ form a basis for the kernel of A_n , so $v_1 + J_n v_1$ and $v_1 - J_n v_1$ also form a basis of the kernel of A_n (one that conveniently splits into a symmetric and antisymmetric part).

Observe that J_n restricted to E^\pm is $\pm I$. Thus, we have, for $s \in E^+$ and $a \in E^-$:

$$\begin{aligned} h_n(A_n, J_n)s &= h_n(A_n, I)s = (A_n^{n+1} - 2A_n^n - 2I)s = f_n(A_n)s, \\ h_n(A_n, J_n)a &= h_n(A_n, -I)a = (A_n^{n+1} - 2A_n^n + 2I)a = g_n(A_n)a. \end{aligned}$$

Thus the minimal polynomial for A_n restricted to E^+ and to E^- are factors of $xf_n(x)$ and $xg_n(x)$, respectively, because $A_n h_n(A_n, J_n) = 0$. Then, since

$$\begin{aligned} A_n(e_{n+2} \pm J_n e_{n+2}) &\neq 0, \\ f_n(A_n)(v_1 + J_n v_1) &\neq 0, \quad g_n(A_n)(v_1 - J_n v_1) \neq 0, \end{aligned}$$

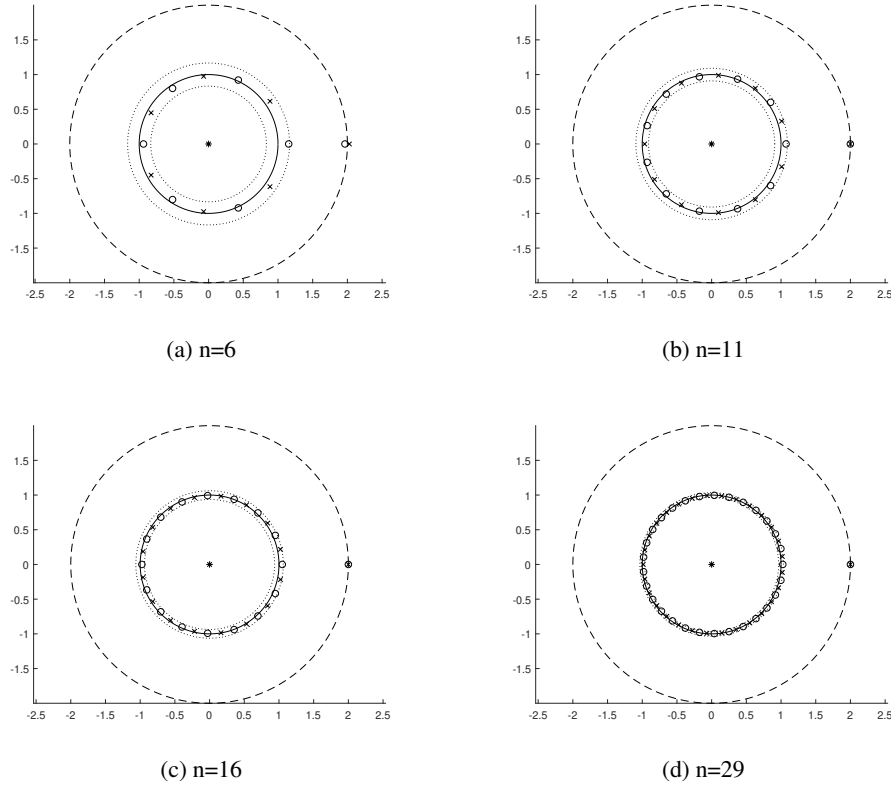


Figure 7. Pictures of the roots of f_n and g_n for different values of n ; roots of f_n are marked with crosses, roots of g_n are marked with circles, and the origin is marked with an asterisk (where A_n has a double eigenvalue). The circle of radius 2 is a dashed line, the unit circle is a solid line, and the circles with radius $1 \pm n^{-1}$ are dotted lines.

we see that the minimal polynomials for A_n restricted to E^+ and E^- must be exactly equal to $xf_n(x)$ and $xg_n(x)$. Then the minimal polynomial for A_n on $\mathbb{C}^{2n+4} = E^+ \oplus E^-$ is the lowest common multiple of the minimal polynomials for A_n on each subspace E^\pm , which means that $m_{A_n}(x) = xf_n(x)g_n(x)$ (as f_n and g_n share no roots). The degree of $m_{A_n}(x)$ is $2n + 3$, but we know that the kernel is two-dimensional, so the characteristic polynomial must be $\chi_{A_n}(x) = xm_{A_n}(x)$, since the degree of $\chi_{A_n}(x)$ is exactly $2n + 4$.

Lastly, the minimal polynomial is separable, by Lemma 6, so we see that A_n is diagonalizable. Since A_n and J_n commute, there is a basis of shared eigenvectors for A_n and J_n . If v is a non-kernel eigenvector for A_n , then as an eigenvector for J_n it is either an element of E^+ or E^- ; when $A_nv = \lambda v$ for λ a root of f_n , then $v \in E^+$ since the minimal polynomial for E^+ is $xf_n(x)$ and λ is not a root of g_n . Similarly, an eigenvector corresponding to a root of g_n is an element of E^- . The proof is complete. ■

We see that A_n has zero as an eigenvalue with multiplicity two, and the non-zero eigenvalues of A_n are the roots of the polynomials f_n and g_n . We will now show that for $n \geq 5$, both f_n and g_n have a real root near 2, one larger and one smaller respectively, and that all of the other roots are found near the unit circle. Figure 7 shows the roots of m_{A_n} for four different n .

Proposition 8. *The polynomial f_n has the spectral radius of A_n , $2 + 2\kappa_n$, as a root, and $\kappa_n \sim \frac{1}{2^n}$. For $n \geq 5$, the polynomial g_n has a real root at $2 - 2r_n < 2$, with $r_n \sim \kappa_n$. For all $n \geq 1$, all other roots of f_n and g_n are outside the circle of radius $1 - n^{-1}$, and for all $n \geq 6$, all other roots of f_n and g_n are inside the circle of radius $1 + n^{-1}$.*

Proof. Observe that substituting $2 + 2\kappa_n$ into f_n yields:

$$\begin{aligned} f_n(2 + 2\kappa_n) &= (2 + 2\kappa_n)^n (2 + 2\kappa_n - 2) - 2 \\ &= 2((2 + 2\kappa_n)^n \kappa_n - 1) = 0, \end{aligned}$$

by the definition of κ_n . To see roughly how big κ_n is, observe that

$$\frac{1}{2^n} > \frac{1}{(2 + 2\kappa_n)^n} = \kappa_n > \frac{1}{(2 + \frac{2}{2^n})^n} = \frac{1}{2^n} \cdot \frac{1}{(1 + \frac{1}{2^n})^n}.$$

Since $(1 + 2^{-n})^n$ converges to 1 as n tends to infinity, we see that $\kappa_n \sim 2^{-n}$.

Next, observe that applying g_n to $2(1 - 2^{-n})$ yields

$$\begin{aligned} g_n(2(1 - 2^{-n})) &= 2^n \left(1 - \frac{1}{2^n}\right)^n \left(2 - 2 \cdot \frac{1}{2^n} - 2\right) + 2 \\ &= -2 \left(1 - \frac{1}{2^n}\right)^n + 2 > 0. \end{aligned}$$

Then, evaluate g_n at $2(1 - (1 + 2n/2^{-n}) \cdot 2^{-n})$ and use Bernoulli's inequality (used here in the form $(1 - x)^n > 1 - nx$ for $0 < x < 1$ and $n \geq 1$):

$$\begin{aligned} g_n \left(2 \left(1 - \left(\frac{1}{2^n} + \frac{2n}{4^n} \right) \right) \right) &= -2^{n+1} \left(1 - \left(\frac{1}{2^n} + \frac{2n}{4^n} \right) \right)^n \left(\frac{1}{2^n} + \frac{2n}{4^n} \right) + 2 \\ &\leq 2 \left(1 - \left(1 - \left(\frac{n}{2^n} + \frac{2n^2}{4^n} \right) \right) \right) \left(1 + \frac{2n}{2^n} \right) \\ &= \frac{2n}{2^n} \left(-1 + \frac{4n}{2^n} + \frac{4n^2}{4^n} \right). \end{aligned}$$

The quantity inside the parentheses is decreasing for $n \geq 2$ and is negative for $n \geq 5$, so by continuity of g_n there exists a root $2 - 2r_n$ of g_n for $n \geq 5$, where $2^{-n} < r_n < 2^{-n} + 2n4^{-n}$. Thus $r_n \sim 2^{-n} \sim \kappa_n$.

Lastly, we use Rouché's Theorem to estimate the other roots of f_n and g_n . Set $a(z) = 2$ and $b_n(z) = z^n(z - 2)$. For $|z| = 1 - n^{-1}$, we have $|z - 2| \leq |z| + 2 = 3 + n^{-1}$ and hence (noting that $(1 - x)^n < (1 + x)^{-n}$ for $0 < x < 1$ and $n \geq 1$):

$$\begin{aligned} |b_n(z)| &= |z|^n |z - 2| \leq \left(1 - \frac{1}{n}\right)^n \left(3 + \frac{1}{n}\right) \\ &< \frac{3 + 1/n}{(1 + 1/n)^n} \leq \frac{3 + 1}{1 + \frac{n}{n}} = 2 = |a(z)|, \end{aligned}$$

where the last inequality came from the first two terms of the Binomial expansion. We apply Rouché's Theorem to see that $a(z)$ and $a(z) \pm b_n(z) = g_n(z), -f_n(z)$ (so

also $f_n(z)$) have the same number of roots inside $|z| = 1 - n^{-1}$: none, because $a(z)$ is constant and therefore has no roots. On the other hand, for $|z| = 1 + n^{-1}$, we have $|z - 2| \geq 2 - |z| = 1 - n^{-1}$, so again using the Binomial expansion (three terms, this time), we get:

$$\begin{aligned} |b_n(z)| &= |z|^n |z - 2| \geq \left(1 + \frac{1}{n}\right)^n \left(1 - \frac{1}{n}\right) \\ &> \left(1 + \frac{n}{n} + \frac{n(n-1)}{2n^2}\right) \left(1 - \frac{1}{n}\right) \\ &= \left(\frac{5}{2} - \frac{1}{2n}\right) \left(1 - \frac{1}{n}\right). \end{aligned}$$

This last quantity is clearly increasing, and for $n \geq 6$ it is larger than $2 = |a(z)|$. Thus, for $n \geq 6$, Rouché's Theorem says that $b_n(z)$ and $b_n(z) \pm a(z) = g_n(z)$, $f_n(z)$ have the same number of roots inside $|z| = 1 + n^{-1}$: n , because the $n + 1$ roots of $b_n(z)$ are 0 with multiplicity n and 2 with multiplicity 1, and 2 is certainly outside the circle of radius $1 + n^{-1}$ if $n \geq 6$. ■

Corollary 9. *For all $n \geq 1$, the spectral radius of A_n is $2(1 + \kappa_n)$, and so the spectral radius of M_n is 1.*

Proof. For $n \leq 5$, one may use a computer to show that the only root of $m_{A_n}(x)$ at least of magnitude 2 is $2 + 2\kappa_n$. For $n \geq 6$, we use Proposition 8 to conclude that the largest eigenvalue is $2 + 2\kappa_n$. The spectrum of M_n is simply the spectrum of A_n scaled by $(2 + 2\kappa_n)^{-1}$, so the spectral radius of M_n is 1. ■

In [5], the application of Proposition 8 is to provide a sharpness result for a general estimate on the exponential mixing rate for a class of non-autonomous dynamical systems that are perturbations of the map T_0 . This computation is reproduced as the following Corollary, and describes how the second-largest eigenvalue $(2 - 2r_n)(2 + 2\kappa_n)^{-1}$ for M_n approaches 1 as n tends to infinity.

Corollary 10. *The second largest eigenvalue for M_n , and hence for P_n , is asymptotically equivalent to $1 - 2\kappa_n$.*

Proof. For $n \geq 6$, we know that the second largest eigenvalue in modulus for A_n is $2 - 2r_n$, so the second largest eigenvalue in modulus for M_n , and thus P_n (by Lemma 1), is $(2 - 2r_n)(2 + 2\kappa_n)^{-1}$. By Proposition 8, we have $r_n = \kappa_n + o(\kappa_n)$. Thus we have:

$$\begin{aligned} \frac{2 - 2r_n}{2 + 2\kappa_n} &= (1 - r_n)(1 + \kappa_n)^{-1} = (1 - \kappa_n + o(\kappa_n))(1 - \kappa_n + o(\kappa_n)) \\ &= 1 - 2\kappa_n + o(\kappa_n). \end{aligned} \quad \blacksquare$$

Remark. We identified J_n as a $(2n + 4)$ -by- $(2n + 4)$ permutation matrix with ones along the anti-diagonal. To add to our knowledge about J_n , we can also identify J_n as a 2-by-2 flip, by using tensor products: $\mathbb{C}^{2n+4} \simeq E^+ \otimes_{\mathbb{C}} \mathbb{C}^2$, and J_n is the flip in the second coordinate.

Remark. In the proof of Proposition 7, we computed the minimal polynomial for A_n by finding invariant subspaces and working with the restrictions of A_n to those subspaces; the relation $A_n(A_n^{n+1} - 2A_n^n - 2J_n) = 0$ reduced to the relations

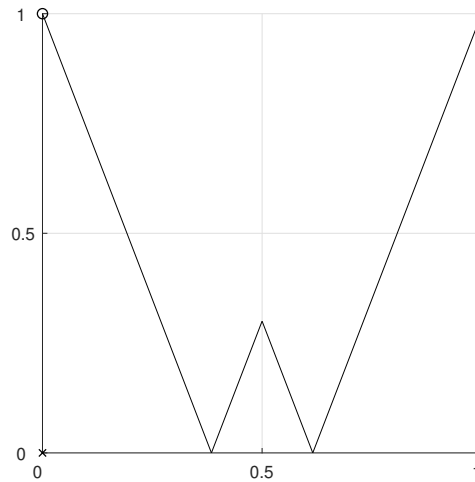


Figure 8. The map \tilde{T}_κ , for $\kappa = 0.3$.

$A_n(A_n^{n+1} - 2A_n^n \mp 2I) = 0$ on the subspaces E^\pm , and these one-matrix relations yielded to standard techniques. However, we also had $J_n^2 = I$, and we could consider the simultaneous equations

$$\begin{aligned} A_n h_n(A_n, J_n) &= A_n(A_n^{n+1} - 2A_n^n - 2J_n) = 0, \\ J_n^2 - I &= 0. \end{aligned}$$

Is it possible to take an algebraic-geometric approach to finding the eigenvalues of A_n and J_n without reducing to the single-variable theory? The answer is yes!

Briefly, by Hilbert's Nullstellensatz we see that the ideal of polynomials in two variables that vanish on the locus of $\{xh_n(x, y), y^2 - 1\}$ is the same as the radical of the ideal \mathcal{J} generated by $\{xh_n(x, y), y^2 - 1\}$. Even better, one can show that \mathcal{J} is actually radical, and that \mathcal{J} is moreover equal to the ideal of polynomials that vanish when evaluated at (A_n, J_n) . Finally, the polynomial $m_{A_n}(x) = xf_n(x)g_n(x)$ is shown to be an element of \mathcal{J} , so we get that A_n is diagonalizable in the same way as before; this means \mathcal{J} is also equal to the ideal of polynomials that vanish on the pairs of eigenvalues (λ, μ) of A_n and J_n . Hence the pairs of eigenvalues are exactly the locus of $\{xh_n(x, y), y^2 - 1\}$, instead of just a subset, and solving for the roots of the two polynomials simultaneously yields the eigenvalues of A_n and the anti/symmetric breakdown. This abstract perspective is another way to see the problem, though our initial proof was much less high-tech. The subsequent computations are not affected by the change.

Spectral Properties of a Related System We may use our knowledge of T_{κ_n} to study a related system. Define $\pi : [-1, 1] \rightarrow [0, 1]$ by $\pi(x) = |x|$ and set $\tilde{T}_\kappa := \pi \circ T_\kappa = |\tilde{T}_\kappa| : [0, 1] \rightarrow [0, 1]$, as depicted in Figure 8. We can ask the same questions about this map: does it have an invariant density? Is it mixing, and if so with what rate? Instead of repeating all of our work, however, we can use the relationship between T_κ and \tilde{T}_κ and the information about T_κ to answer these questions, again by reducing the computations to painless matrix relations.

Observe that because T_κ is odd, for any $x \in [-1, 1]$ we have that T_κ maps $\{\pm x\}$ to $\{\pm T_\kappa(x)\}$. Looking at $\{\pm x\}$ as an equivalence class under $x \sim -x$, we see that the map π defined above collapses each class to a single point in $[0, 1]$: the shared absolute value of the elements of the class. From the definition of \tilde{T}_κ , then, it is clear that $\pi \circ T_\kappa = \tilde{T}_\kappa \circ \pi$.

In addition, for each $n \geq 1$, $\tilde{T}_n := \tilde{T}_{\kappa_n}$ is still Markov. The Markov partition is not quite the same as the partition on $[0, 1]$ for T_n ; the map is no longer monotonic on just two intervals, but rather four intervals. However, we can easily guess a partition; the interval R_{n+4} should be split in two. Note that $1 - \kappa_1 = \frac{1}{2} + \frac{\kappa_1}{2(1+\kappa_1)}$ and for all $n \geq 2$, $\tilde{T}_n^{-1}(\kappa_n) = \frac{1}{2} + \frac{\kappa_n}{2(1+\kappa_n)}$; this point is the zero of \tilde{T}_n larger than $1/2$, and the symmetric point $\frac{1}{2} - \frac{\kappa_n}{2(1+\kappa_n)}$ is the zero smaller than $1/2$.

Lemma 11. *The map \tilde{T}_n is Markov for each $n \geq 1$. For $n = 1$, the Markov partition is*

$$\left\{ (0, \kappa_1), (\kappa_1, \frac{1}{2}), (\frac{1}{2}, 1 - \kappa_1), (1 - \kappa_1, 1) \right\}$$

and for $n \geq 2$, the Markov partition is

$$\left\{ (0, \kappa_n), \left(\kappa_n, \frac{1}{2} - \frac{\kappa_n}{2(1+\kappa_n)} \right), \left(\frac{1}{2} - \frac{\kappa_n}{2(1+\kappa_n)}, \frac{1}{2} \right), \left(\frac{1}{2}, \frac{1}{2} + \frac{\kappa_n}{2(1+\kappa_n)} \right) \right\} \\ \cup \left\{ \left(\tilde{T}_n^{i+1}(\kappa_n), \tilde{T}_n^i(\kappa_n) \right) \right\}_{i=1}^{n-2} \cup \left\{ \left(\tilde{T}_n(\kappa_n), 1 \right) \right\}.$$

The Markov partition has, in all cases, $n + 3$ intervals.

Proof. We again apply Lemma 2. For $n = 1$, the Markov partition is simply the (interiors of the) intervals of monotonicity, since $\tilde{T}_1(\kappa_1) = 0$ and $\tilde{T}_1(1/2) = \kappa_1$; clearly, there are $4 = 1 + 3$ intervals. For $n \geq 2$, the point $\frac{1}{2} - \frac{\kappa_n}{2(1+\kappa_n)}$ is mapped to 0, and the remainder of the points are just as in the case of T_{κ_n} . Because we have split one of the intervals in $[0, 1]$ in two (but are only considering $[0, 1]$, not $[-1, 1]$), there are exactly $n + 3$ elements in the Markov partition. ■

The Markov partitions for $n = 1, 4$ are illustrated in Figure 9. We will denote the intervals in order left-to-right by $\{S_1\}_1^{n+3}$. For $n \geq 4$ the general form of the adjacency matrix B_n is as in Figure 10. For $n \leq 3$ some of the columns are combined. Observe that B_n is almost identical to the bottom-right quadrant of A_n , with the exception of an extra column; this is expected, given how we modified the Markov partition by splitting R_{n+4} into S_2 and S_3 while leaving the other intervals the same.

We now compute the spectral data for B_n . Towards this goal, for notation let \tilde{V}_n be the span of the functions $\{\mathbb{1}_{S_i}\}_{i=1}^{n+3}$, and let $\tilde{\phi} : \tilde{V}_n \rightarrow \mathbb{C}^{n+3}$ be the isomorphism from Lemma 1 with $\tilde{\phi}(\mathbb{1}_{S_i}) = d_i$. Our proof will run through the action of A_n on E^+ ; for each i between 1 and $n + 2$, let $s_i = \frac{1}{2}(e_{n+3-i} + e_{n+2+i})$, and observe that $\{s_i\}_{i=1}^{n+2}$ is a basis for E^+ . Then, call $C_n : \mathbb{C}^{n+2} \rightarrow \mathbb{C}^{n+2}$ the matrix representation of A_n on $E^+ = \text{span}_{\mathbb{C}}\{s_i\}_{i=1}^{n+2}$. Moreover, let ι be the matrix representations of the inclusion of E^+ into \mathbb{C}^{n+3} by splitting up s_2 into $d_2 + d_3$, as pictured in Figure 11, so that $\iota(s_1) = d_1$, $\iota(s_2) = d_3 + d_4$, and $\iota(s_k) = d_{k+1}$ for $k \geq 3$.

Proposition 12. *Let $n \geq 1$. We have:*

1. $\iota C_n = B_n \iota$, with C_n as given in Figure 12;

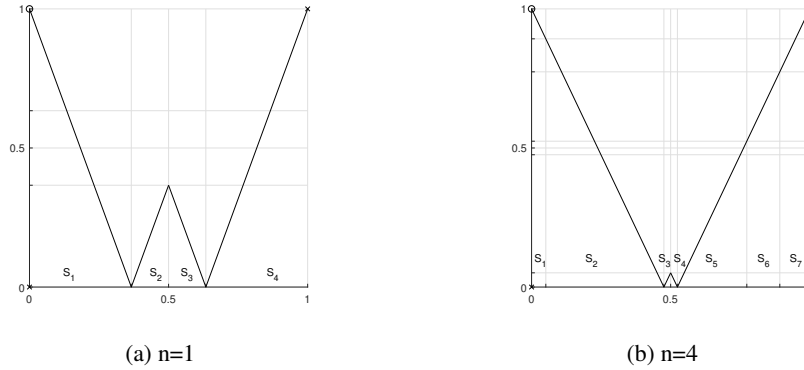


Figure 9. Markov partitions for \tilde{T}_n , for $n = 1, 4$.

$$\begin{bmatrix}
 0 & 1 & 1 & 1 & 1 & 0 & & 0 & 0 \\
 0 & 1 & 0 & 0 & 1 & 0 & & 0 & 0 \\
 0 & 1 & 0 & 0 & 1 & 0 & \dots & 0 & 0 \\
 0 & 1 & 0 & 0 & 1 & 0 & & 0 & 0 \\
 0 & 1 & 0 & 0 & 0 & 1 & & 0 & 0 \\
 & & \vdots & & & & \ddots & & \\
 0 & 1 & 0 & 0 & 0 & 0 & & 1 & 0 \\
 0 & 1 & 0 & 0 & 0 & 0 & & 0 & 1 \\
 1 & 0 & 0 & 0 & 0 & 0 & & 0 & 1
 \end{bmatrix}$$

Figure 10. General form of the $(n+3)$ -by- $(n+3)$ adjacency matrix B_n .

$$\begin{bmatrix}
 1 & 0 & 0 & & 0 \\
 0 & 1 & 0 & & 0 \\
 0 & 1 & 0 & & 0 \\
 0 & 0 & 1 & & 0 \\
 & & & \ddots & 0 \\
 0 & 0 & 0 & & 1
 \end{bmatrix}$$

Figure 11. The $(n+3)$ -by- $(n+2)$ matrix ι , representing the inclusion $E^+ \rightarrow \mathbb{C}^{n+3}$.

2. the kernel of B_n is $\ker(B_n) = \text{span}_{\mathbb{C}}\{(d_3 - d_4), (d_1 + d_2 - (d_5 + \dots + d_{n+3}))\}$;
3. the minimal polynomial for B_n is $\min_{B_n}(x) = x f_n(x)$;
4. the characteristic polynomial for B_n is $\text{char}_{B_n}(x) = x^2 f_n(x)$;
5. B_n is diagonalizable, the spectral radius of B_n is $2 + 2\kappa_n$, and all of the other eigenvalues of B_n are zero or near the unit circle. The eigenvector corresponding to the spectral radius is $\iota(w)$, where $w \in E^+$ is the eigenvector corresponding to the spectral radius for C_n .

Proof. First, note that the action of A_n restricted to E^+ can be seen as identifying the

$$\begin{bmatrix} 0 & 2 & 1 & 1 & & 0 & 0 & 0 \\ 0 & 1 & 0 & 1 & & 0 & 0 & 0 \\ 0 & 1 & 0 & 1 & & 0 & 0 & 0 \\ & \vdots & & & \ddots & \vdots & & \\ 0 & 1 & 0 & 0 & & 1 & 0 & 0 \\ 0 & 1 & 0 & 0 & & 0 & 1 & 0 \\ 0 & 1 & 0 & 0 & & 0 & 0 & 1 \\ 1 & 0 & 0 & 0 & & 0 & 0 & 1 \end{bmatrix}$$

Figure 12. The $(n+2)$ -by- $(n+2)$ matrix C_n , representing the action of A_n on E^+ .

vectors e_i and e_{2n+5-i} and looking at the action of A_n on the vectors e_{n+3} to e_{2n+4} , because $E^+ = \text{span}_{\mathbb{C}}\{s_i\}_{i=1}^{n+2}$ with $s_i = \frac{1}{2}(e_{n+3-i} + e_{n+2+i})$. The columns of the matrix A_n indicate the images under T_n of the intervals R_i for each i , and so the columns of the restriction C_n indicate the images under T_n of the intervals R_{n+3} up to R_{2n+4} under the identification of R_i with R_{2n+5-i} (considered with multiplicity). However, this is exactly what the columns of B_n indicate, because B_n is the adjacency matrix for \tilde{T}_n , taken with the refined partition $\{S_i\}_{i=1}^{n+3}$. Since ι represents the refinement of the partition, we have $\iota C_n = B_n \iota$. From this equality we can obtain the remainder of the results in Proposition 12.

Looking at \tilde{T}_n , it is clear that the kernel of B_n is equal to $\text{span}_{\mathbb{C}}\{(d_3 - d_4), (d_1 + d_2 - (d_5 + \cdots + d_{n+3}))\}$, because these two vectors represent the two facets of symmetry in \tilde{T}_n (the symmetry in the long branches and the symmetry in the short branches).

To find the minimal polynomial for B_n , recall from Proposition 7 that the minimal polynomial for A_n restricted to E^+ is equal to $x f_n(x)$. Thus, we have

$$B_n f_n(B_n) \iota = \iota C_n f_n(C_n) = 0,$$

since C_n represents A_n acting on E^+ and so satisfies the minimal polynomial. We also have that

$$\mathbb{C}^{n+3} = \text{Im}(\iota) \oplus \text{span}_{\mathbb{C}}\{d_3 - d_4\},$$

because ι is injective (with rank $n+2$) and $d_3 - d_4$ is not in the image of ι . Since $B_n f_n(B_n)$ annihilates both the image of ι and $d_3 - d_4$ but $f_n(B_n)(d_3 - d_4) = -2(d_3 - d_4)$ and $B_n(d_1) \neq 0$, we see that the minimal polynomial of B_n is $m_{B_n}(x) = x f_n(x)$. The characteristic polynomial for B_n is $\chi_{B_n}(x) = x^2 f_n(x)$, of course, because the kernel of B_n is two-dimensional and the degree of $\chi_{B_n}(x)$ is $n+3$.

Finally, the minimal polynomial for B_n is separable, so B_n is diagonalizable. By Proposition 8, the largest eigenvalue of B_n is $2 + 2\kappa_n$, and all other eigenvalues of B_n zero or near the unit circle (asymptotically). If $w \in E^+$ is the eigenvector corresponding to $2 + 2\kappa_n$ for C_n , then

$$B_n(\iota(w)) = \iota(C_n w) = (2 + 2\kappa_n)\iota(w),$$

so $\iota(w)$ is the eigenvector for B_n corresponding to $2 + 2\kappa_n$. ■

Observe that B_n shares no eigenvalues corresponding to the antisymmetric eigenvectors for A_n ; this makes sense, since the map π collapsed all of those vectors to 0, and we are left with the symmetric eigenvectors. It did, however, introduce a new kernel vector, by introducing a new aspect of symmetry.

In addition, note that we could not simply apply Lemma 1 with the matrix C_n , because \tilde{T}_n is not Markov with respect to the partition $\{R_i\}_{i=n+3}^{2n+4}$. However, the relationship between C_n and B_n allowed us to painlessly translate facts about A_n (and C_n) into facts about B_n , the actual adjacency matrix for \tilde{T}_n .

Corollary 13. *The second-largest eigenvalue of the Perron-Frobenius operator for \tilde{T}_n has modulus at most $(1 + n^{-1})(2 + 2\kappa_n)^{-1}$ (for $n \geq 6$), which is asymptotically equivalent to $\frac{1}{2}(1 + n^{-1})$.*

Proof. The spectral radius of B_n is still $2 + 2\kappa_n$, by Corollary 9 and Proposition 12, so the spectral radius of the Perron-Frobenius operator for \tilde{T}_n is 1 and the second-largest eigenvalue has modulus at most $1 + n^{-1}$ divided by $2 + 2\kappa_n$, using Proposition 7 to get the upper bound. We then have (since $\kappa_n \sim 2^{-n}$):

$$\begin{aligned} \frac{1 + n^{-1}}{2(1 + \kappa_n)} &= \frac{1}{2} \left(1 + \frac{1}{n}\right) (1 - \kappa_n + o(\kappa_n)) \\ &= \frac{1}{2} \left(1 + \frac{1}{n} - \kappa_n + o(\kappa_n)\right) = \frac{1}{2} \left(1 + \frac{1}{n} + o\left(\frac{1}{n}\right)\right), \end{aligned}$$

which shows that $(1 + n^{-1})(2 + 2\kappa_n)^{-1}$ is asymptotically equivalent to $\frac{1}{2}(1 + n^{-1})$. ■

Conclusion for Mixing Times At the beginning of this paper, we asked about mixing times and mixing rates for dynamical systems. We can now answer that question for our two systems, T_n and \tilde{T}_n . For T_n , we have shown that the second-largest eigenvalue of the Perron-Frobenius P_n is approximately $1 - 2\kappa_n$ (Corollary 10 and Lemma 1). Thus the mixing time for T_n is, ignoring a scale factor,

$$\frac{1}{|\log(1 - 2\kappa_n)|} \sim \frac{1}{2\kappa_n} \sim 2^{n-1},$$

using the fact that $\kappa_n \sim 2^{-n}$.

On the other hand, for \tilde{T}_n , Corollary 13 says that the second-largest eigenvalue of the Perron-Frobenius operator has modulus at most $(1 + n^{-1})(2 + 2\kappa_n)^{-1}$. By a similar computation, the mixing time for \tilde{T}_n (with $n \geq 6$) is $O(1)$, which is much smaller than the mixing time for T_n .

This result matches our intuition: for T_n , taking the perturbation to zero (or n to infinity) leads to no mixing between the two halves, so the mixing time should tend to infinity, whereas for \tilde{T}_n , taking the perturbation to zero leads to a mixing tent map, and hence the mixing time should approach that for the unperturbed map. The difference in the orders of the mixing times indicates significant dynamical information about how these two systems are distinct, and we obtained this information by performing calculations with matrices (without touching the matrices themselves) and some analysis of roots of polynomials.

ACKNOWLEDGEMENTS: The author would like to thank Anthony Quas for the prodding to consider how elegant and satisfying this collection of ideas really is.

REFERENCES

1. S. Axler. Down with determinants! *Amer. Math. Monthly*, 102(2):139–154, 1995.
2. M. Blank and G. Keller. Random perturbations of chaotic dynamical systems: stability of the spectrum. *Nonlinearity*, 11(5):1351–1364, 1998.
3. A. Boyarsky and P. Góra. *Laws of chaos*. Probability and its Applications. Birkhäuser Boston, Inc., Boston, MA, 1997. Invariant measures and dynamical systems in one dimension.
4. J. Ding, Q. Du, and T. Y. Li. The spectral analysis of Frobenius-Perron operators. *J. Math. Anal. Appl.*, 184(2):285–301, 1994.
5. J. Horan. Asymptotics for the second-largest lyapunov exponent for some Perron-Frobenius operator co-cycles. Preprint: <https://arxiv.org/abs/1910.12112>.
6. R. A. Horn and C. R. Johnson. *Matrix analysis*. Cambridge University Press, Cambridge, second edition, 2013.
7. D. A. Levin, Y. Peres, and E. L. Wilmer. *Markov chains and mixing times*. American Mathematical Society, Providence, RI, 2009. With a chapter by James G. Propp and David B. Wilson.
8. W. A. McWorter, Jr. and L. F. Meyers. Computing eigenvalues and eigenvectors without determinants. *Math. Mag.*, 71(1):24–33, 1998.

JOSEPH HORAN is a Ph.D. candidate at the University of Victoria, for now. He is interested in dynamical systems, ergodic theory, and mathematics education, and is very excited to see beautiful mathematics.

Department of Mathematics and Statistics, University of Victoria, Victoria, BC, Canada V8P 5C2
jahoran@uvic.ca